

Flux potentials of local talc in low voltage electro-porcelain insulator production

Ifeanyi Uchegbulam^{*1,a}, Agbo Sunday Chukwuemeka^{2,b}, Onyinyechi Pauline Elenwo^{3,c}, Emmanuel Owoichoечи Momoh^{4,d}

¹Production Tech., School of Science Laboratory Technology, University of Port Harcourt, Choba, Nigeria

²Ceramics Research and Production Department, Projects Development Institute (PRODA) Enugu, Nigeria

³Physics Department, Faculty of Science, University of Port Harcourt, Choba PMB 5323, Nigeria

⁴Faculty of Environment Science and Economy, University of Exeter, Streatham Campus, Exeter, UK

Article Info

Abstract

Article history:

Received 04 Dec 2023

Accepted 22 Mar 2024

Keywords:

Ceramic;

Porcelain insulator;

Talc;

Feldspar;

Sintering;

Voltage

Increasing demand for accessories like porcelain electric insulators have continued in developing countries causing overdependence on imported products. Meanwhile, raw materials for their local production are available in commercial quantities with high firing temperature being the major challenge. Hence, the need for fluxing agents that can reduce the working temperature led to the investigation of Talc as a partial replacement of conventional Feldspar. An optimum replacement of 10% Feldspar with Talc was adopted, and this recipe showed microstructurally enriched glassy phase, primary and secondary Mullite with other crystalline phases like Cristobalite, Microcline and Albite at 1200°C with micropores evident in both the Talc and Feldspar formulations. The produced insulator fired at 1200°C offered an optimum thermal conductivity of 0.2768W/mK with reductions in water absorption, apparent porosity and linear shrinkage by 78.29%, 76.02% and 19.75% respectively with a 9.48% rise in bulk density. The electrical performance comprised Inception, Withstand and Breakdown Voltages of 10.2 kV, 14 kV and 20 kV respectively at leakage currents of 0.2 mA, 1.2 mA and 2 mA accordingly. With a withstand voltage above 11 kV and breakdown voltage below 22 kV, this pin-type porcelain insulator will find wide application in both electric substations and end user load points like commercial and residential electric power lines. The novelty lies on the fluxing and filler potentials of Talc as a locally-sourced mineral in porcelain insulator production which increases the market value of Nigerian Talc while reducing importation, costs of energy and raw materials in porcelain production.

© 2024 MIM Research Group. All rights reserved.

1. Introduction

Porcelain is one of the engineering materials that have passed through ages without losing its relevance despite the development of modern plastic and glassy materials. This sustained significance can be linked to its durability and adaptability to harsh environmental situations. They are extensively used for chemical, heat and electrical resistant purposes. Their mechanical properties, corrosion resistance, low water affinity, high heat resistance, and high electrical resistivity are responsible for their excellent performance in refractories, laggings, tiles, kitchen and sanitary wares.

They also demonstrate excellent chemical resistance (as laboratory wares), thermal shock (as pestles), beautiful textures (when glazed for decorative uses) as well as fatigue

*Corresponding author: uche.berdeen.ac.uk@gmail.com

^a orcid.org/0000-0002-0836-3370; ^b orcid.org/0000-0002-7803-0950; ^c orcid.org/0009-0009-7226-9635;

^d orcid.org/0000-0003-3432-1366

DOI: <http://dx.doi.org/10.17515/resm2024.96ma1204rs>

Res. Eng. Struct. Mat. Vol. x Iss. x (xxxx) xx-xx

resistance (in dentistry). As non-conductors of electricity, porcelain insulators find satisfactory usage in unlimited indoor electrical applications as well as outdoor uses as high voltage insulations like overhead power transmission and distribution lines, bushings for transformers, etc.

In service, a Porcelain Electric Insulator is exposed to very harsh environmental conditions like heat, rain, humidity, dust etc. For instance, while establishing the need for formulating a corrosion control protocol for insulators, it was noticed in [1] that relative humidity plays key roles in insulator electrolytic corrosion. Similarly, in [2], it was reported that corrosion of porcelain insulating systems are mainly dependent on geographic locations with the cap components of the insulators degrading by galvanic corrosion mechanism while the pin corrodes by both crevice and electrolytic corrosion mechanisms. Other studies such as [3], studied the biological contamination of electrical insulators by alga *Chlorella vulgaris*. Their findings showed the adverse effect of bio-contamination which reduced the flashover voltage by 12% and increased the leakage currents up to 80%. In [4], artificial neural network was used to predict the flashover voltage of humidity and pollution induced surface contaminations of porcelain insulators.

These challenges have motivated researchers and scientists to investigate diverse improvement techniques to enhance the performance of Porcelain insulators through material formulations and production methods. Since sintering temperature also known as firing or working temperature complemented with formulation recipe are the principal factors responsible for the precipitation of crystalline phases, which in turn dictates the properties of porcelain materials, it becomes imperative to understand the relationship between these factors for performance optimization. Several authors have investigated the partial replacement and variation of the amount of quartz, Feldspar, kaolin and ball clay in porcelain recipes. In [5], the use of micro additives as fillers to enhance the electrical properties of ceramic-glass insulators was studied while [6], used recycled waste glass from broken car glasses as a replacement of K-Feldspar for the production of porcelain. Their findings showed improvements in microhardness and dielectric properties. Remarkably, [7] in their use of cullet to substitute the Feldspar component found that this measure offered excellent dielectric strength at a lower kiln temperature. Similarly, the partial replacement of Feldspar with sodium bicarbonate has also been reported in [8], which reduced sintering temperature and improve dielectric performance of porcelain insulators. Mineral raw materials are potential substitutes to the feldspathic component of porcelain formulation. These materials like Talc have been used for other industrial purposes and is both available and affordable in commercial quantities in Nigeria. Talc is a soft and light-weight mineral with its mineralogical occurrence mainly from the metamorphosis of other rocks. It is a secondary mineral from either carbonate of magnesium like dolomite and magnesite or oxides of silicon such as serpentine and tremolite. This is why it is generally recognized as hydrated magnesium silicate $Mg_3Si_4O_{10}(OH)_2$ [9,10]. It has several uses ranging from cosmetics, agriculture, industrial lubrication, electrical wire insulation and even anticaking agent in drug tablets molding. It is a soft and whitish mineral when ground. The physico-chemical properties like softness, hydrophobicity, low thermal and electrical conductivity with high crystallinity and specific surface area of Talc suggest its suitability as a fluxing material in porcelain production. Talc as a magnesium-rich phyllosilicate has found extensive industrial applications for making plastics, detergents, paint, paper, pharmaceuticals, pesticides, rubber, cosmetics, ceramics, adhesives, part of animal feed and acts as a hydroTalcite in the petroleum industry [11-13].

Hence, in this study, the use of Talc as a partial replacement of Feldspar in formulation of porcelain insulator recipes and how this affects the physical properties, thermal stability and electrical performance of the insulator were investigated.

2. Materials and Methods

2.1 Material characterization

The raw materials were obtained from local Nigerian communities: Kaolin from the Projects Development Institute’s mineral store, Talc from Kenyatta Industrial market and Silica from Iva Pottery all in Enugu state while the Ball clay was obtained from Ehime Mbano in Imo state and Feldspar from Okene in Kogi state. These materials were identified at the Projects Development Institute at minimum purity levels of 97.3%, 98.5%, 97.4% and 95.8% for Kaolin, Talc, Silica and Ball clay respectively. The methodology employed in this study is illustrated in the overview of Figure 1.

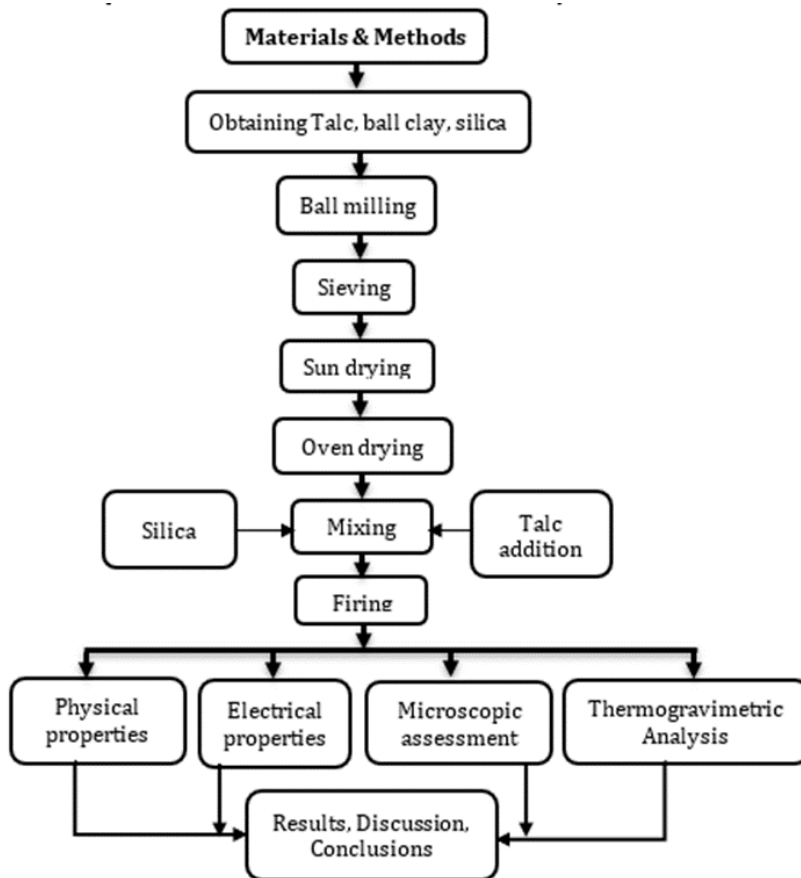


Fig. 1. Overview of the study

2.2 Slip formulation and Molding into Porcelain Insulator

The kaolin, ball clay and silica were in fixed amounts of 40%, 10% and 25% respectively, while Feldspar and Talc were varied as shown in Table 1. These starting materials were obtained as lumpy coarse powders and were crushed in a ball mill to obtain finer particle sizes.

Further processing was carried out by soaking in distilled water, vigorous stirring to achieve adequate dissolution, and filtering (through a 0.425 mm mesh sieve) to get rid of organic matter. This procedure was followed by allowing the sediments to settle. The

floated water was then run off to isolate other suspended solids and residual organic matter after which the condensed clay was sun-dried for 5 hours prior to oven drying at 100 °C for 3 hours. The dried clay was later pulverized and sifted through a 0.18mm sieve. With the recipe in Table 1, 1.6kg of the clay sample was used as the base raw material with the other materials added to achieve different slurries. The sample codes are shown in Table 1. Subsequently, 2g of Sodium Silicate (Na_2SiO_3) was added to each blended mixture of powders in order to inhibit flocculation of suspended solids. The powders were then kneaded in appropriate amount of water into plastic slip until ready for molding.

Table 1. Formulation of Porcelain insulator

Code	Kaolin	Ball clay	Silica	Feldspar	Talc
A	40	10	25	25	0
B	40	10	25	23	2
C	40	10	25	21	4
D	40	10	25	19	6
E	40	10	25	17	8
F	40	10	25	15	10

With these conditions, the slip was poured into a plaster-of-Paris mold consistent with the industrial dimensions of porcelain insulators. The slip was poured until the mold gate was full. Extra slip was added after two hours to supplement mass reduction due to absorbed water. The mold was left to set for 5 hours, after which the cast porcelain was removed from the mold and fettled to obtain a smooth surface finish.

The green compacts were oven dried at 120°C for 2 hours to get rid of mechanically bound water prior to Bisque firing up to 900°C for 3 hours to obtain the adequate porcelain sinter following the procedure conducted in [14]. To achieve the characteristic brown colored impervious glaze, the fired bisques were immediately dipped into a glaze slurry made from Feldspar, Silica, clay, borax, zinc oxide and cobalt oxide. The dipping process was carried out by immersing the fettled green compact into a container of the glaze compound. The glaze-coated compact was sun-dried for 2 hours and fired up to 900°C for 1 hour and allowed to cool under ambient conditions. This glazing process was repeated to ensure high glaze penetration and adherence on the fettled surface. This was followed by a Gloss-firing at 1200°C in an electric kiln at a ramp of 5°C/min and dwell time of 150 minutes. The sintered porcelain products were allowed to cool to room temperature within the kiln for about 15 hours after which the produced porcelain insulators were taken out of the kiln. Industrial sized samples were made so that their properties can be compared to those of commercial products in the market.



Fig. 2. The produced porcelain insulators at different levels of glazing

2.3 Molding of Test Pieces and The Porcelain Insulator

To mold test pieces for physical analysis, three metallic molds were used. The molds were firstly lubricated for ease of retrieving of the green compact. Different mold patterns were produced: the cylindrical patterns of 3.5 ϕ x 3 cm, and short rectangular patterns of 8 x 4 x 1.5 cm while the longer rectangular patterns were of 9.5 x 2 x 1.5 cm. Three (3) samples each of the three sets of test pieces were used for the physical analyses.

2.4 Physical Analysis

Physical properties such as making water, water absorption, porosity, shrinkage, apparent and bulk density of the pellets at different firing temperatures were analyzed in accordance with the requirements of ASTM C20-00 [15], for water absorption, apparent porosity, apparent density, and bulk density.

2.4.1 Making Water

The making water is a very important parameter in slip casting as it represents the amount of water needed to make a plastic slip from the mixture of raw materials. In this study, the making water was determined by weighing the cylindrical test pieces immediately after molding and this weight was recorded as the wet weight (w_o). After this, the test pieces were air-dried for 24hrs, then oven-dried at 105°C until a constant weight was recorded as W_i . The making moisture was then estimated from Eq. 1.

$$\text{Making Moisture (\%)} = \frac{W_o - W_i}{W_o} \times 100 \quad (1)$$

2.4.2 Water Absorption

As a vital parameter, the water absorption (W_a) which demonstrates the extent of curing of the porcelain when fired was also evaluated. This was carried out by measuring the post-drying weight (w_d). The post-dried samples were then soaked in water for 1 hour, cleaned and reweighed as weight after soaking in water as (w_w). Eq. 2 was used to evaluate the water absorption of the samples.

$$W_a (\%) = \frac{W_w - W_d}{W_d} \times 100 \quad (2)$$

2.4.3 Apparent Porosity

The void composition of porcelain insulator largely affects their dielectric strengths. Both accessible and remote pores make up the total porosity of porcelain products.

The apparent porosity test was carried out in accordance with the requirement of ASTM C20-00, (2015), [15]. The samples were suspended in a beaker of water, with their weights measured via a lever balance. The suspended weight was recorded as W_s while the dry weight w_d and the wet weight w_w were measured in line with the procedure described in section 2.4.2. Eq. 3 was used to evaluate the apparent porosity of the samples.

$$\text{Apparent Porosity (\%)} = \frac{W_w - W_d}{W_w - W_s} \times 100 \quad (3)$$

2.4.4 Shrinkage

The linear shrinkage of ceramic products could lead to excessive dimensional instability, thereby, adversely affecting the performance of the finished product. Therefore, analysis of shrinkage is very important in the design of ceramic components. In this study, the shrinkages of the samples were estimated by measuring the sample lengths before and after kiln firing in line with ASTM C356-17, [16]. A vernier caliper was used to insert a 0.5 cm mark on each of the rectangular test pieces and this was recorded as the original length L_o (in cm). The test pieces were then sun-dried outdoor in still air for 7 days. The samples were then transferred into an oven and at 105°C until a constant weight was obtained. The contraction from the 5cm mark was recorded as the dried length, L_d (in cm). Finally, the dried samples were fired to sintering temperatures. The determination of shrinkage was conducted for samples kiln-fired at 1000°C and 1200°C while the shrinkage of the test pieces was determined by measuring the change in the distance between the initial 5 mm markings. The final length after firing was recorded as the fired length, L_f (in cm). The different variants of the shrinkage were then estimated using Eqs. 4, 5 and 6. This procedure was consistent with other studies [14, 17].

$$\text{Wet - Dry Shrinkage (\%)} = \frac{L_o - L_d}{L_o} \times 100 \quad (4)$$

$$\text{Dry - Fired Shrinkage (\%)} = \frac{L_d - L_f}{L_d} \times 100 \quad (5)$$

$$\text{Total Shrinkage (\%)} = \frac{L_o - L_f}{L_o} \times 100 \quad (6)$$

2.4.5 Apparent and Bulk Density

The apparent and bulk densities of the samples were estimated using Eqs 7 and 8 following the procedure described in sections 2.4.2 and 2.4.3. Table 4 presents the results of the apparent and bulk densities of the samples.

$$\text{Apparent Density (\%)} = \frac{W_d}{W_d - W_s} \times 100 \quad (7)$$

$$\text{Bulk Density (\%)} = \frac{W_d}{W_w - W_s} \times 100 \quad (8)$$

Where W_d , W_s and W_w are previously defined in sections 2.4.2 and 2.4.3.

2.5 Microscopic Evaluation

The samples were polished with a moist emery cloth, cleaned and sun-dried prior to microscopic examination using Keyence VH-Z450/VH-6300 Digital Microscope with VH-Z450 High-Range Zoom Lens at 500X magnification.

2.6 Thermal Analysis

The thermal property of the clay samples was analyzed with Shimadzu DTG-60H model (TA Instruments, USA) using differential scanning calorimetry (DSC) and a simultaneous thermal analyzer (Differential Thermal Analysis-Thermogravimetric Analysis, DTA/TGA). The DTG procedure was carried out by heating the clay samples from room temperature to 1200 °C at a ramp of 10 °C/min under a steady air flow of 50 ml/h. A 3.002mg sample was introduced into a Platinum cup, heated in comparison to a reference crucible and cooled at instrument cooling rate to obtain DSC and DTA/TGA curves that reveal the

thermal profiles at different mineralogical transformation during the firing of the produced insulator.

2.7 Electrical Analysis

The main aim of the electrical analysis on the porcelain bodies was to determine their insulating properties. The parameters tested were the dielectric inception voltage, withstand voltage and breakdown voltage as well as the leakage currents at these various voltage limits. These were carried out using BAUR PGK 260 HB AC/DC HV test set, Austria, by applying electrodes at the ends of the porcelain insulator and results presented in section 3.6.

3. Results and Discussion

3.1 Material Characterization

This result of chemical composition (see Table 2) shows that silica (SiO₂) and alumina (Al₂O₃) are the principal oxides found in the raw materials while other oxides were present in negligible quantities. This result agrees with findings in [7] and [18]. Remarkably, flux content in Feldspar (K₂O-Na₂O) sums up to 13.21% which is greater than the 12% threshold [18] for porcelain insulators. Also, the high potash and soda contents of the Feldspar with low lime composition shows that the Feldspar is not a “lime Feldspar”.

Table 2. Chemical composition of the starting raw materials in % oxide constituents

Component (%)	Kaolin Clay	Feldspar	Iva-pottery sand
SiO ₂	60.0	64.65	74.15
Al ₂ O ₃	21.0	16.1	13.73
Fe ₂ O ₃	0.5	1.86	0.005
Na ₂ O	0.031	2.99	-
K ₂ O	0.75	10.22	-
TiO ₂	0.9	1.4	1.3
LOI	11.34	1.62	0.61

3.2 Water Absorption, Making Water and Apparent Porosity

As the Talc content increased from 0 to 10% and were fired up to 1000 °C, it was observed that the apparent porosity was gradually increasing. This may be due to the linear expansion that occurred within 1000 °C causing crack nucleation, thereby, adding to the micropore density (i.e., the number of micropores per unit volume of porcelain).

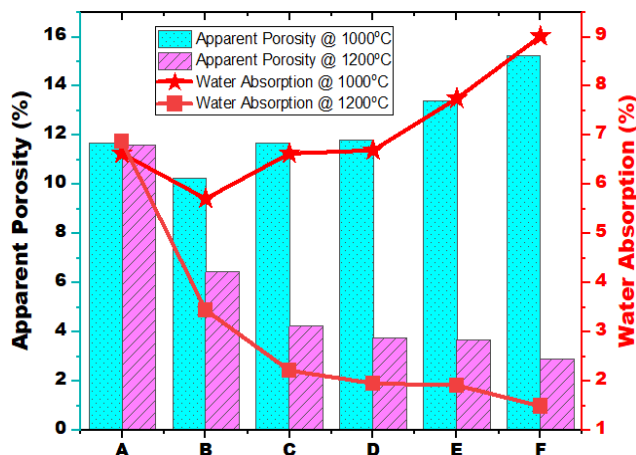


Fig. 3. Apparent porosity and water absorption of PPE insulator as functions of firing temperature (1000 - 1200°C)

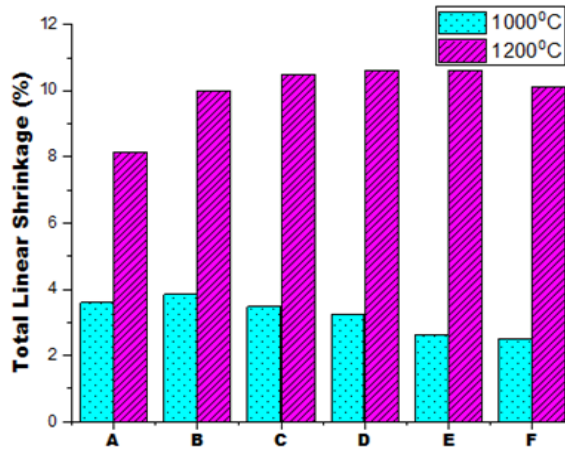
However, as the firing temperature was increased to 1200°C, a significant reduction in apparent porosity, was observed. Evidently, these pores collapse as most of the porcelain materials melt at temperatures above 1000°C. Figure 3 revealed that water absorption increased at 1000°C but reduced at 1200°C. This indicates that there is a correlation between porosity and water absorption such that increase in apparent porosity creates more pores that causes water ingress, hence, increases water absorption. Conversely, as the apparent porosity reduces, there are less pore spaces to accommodate absorbed water thereby causing the reduction in the percentage water absorption. Figure 3 also revealed that the 10% Talc concentration offered the least porosity and water absorption at 1200°C due to the reduced apparent porosity from 12.09 % in the Feldspar-rich recipe to 2.90 % in 10% Talc substitution and a consequent 76.02 % reduction in apparent porosity. In addition, water absorption was reduced from 6.88 % in the Feldspar-rich recipe to 1.49 % in the 10 % Talc substitution resulting in a 78.29 % reduction in water absorption. This trend in reduction of both apparent porosity and water absorption at higher temperatures is consistent with previous studies [7, 19].

3.3 Linear Shrinkage, Apparent and Bulk Density

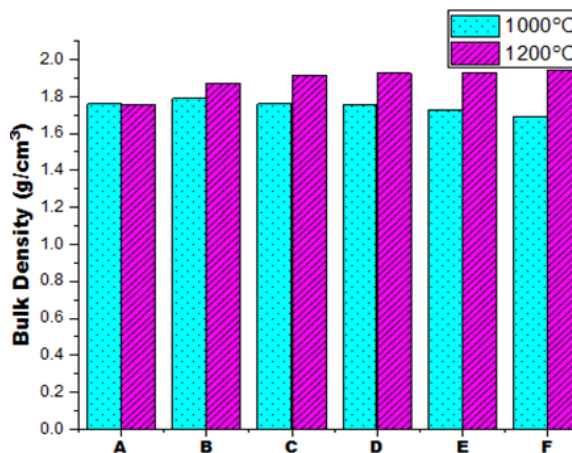
At 1000°C, the linear shrinkage increased until 6% Talc but then decreased as the Talc content approached 10 % (see Figure 4 (a)). As temperature increased, release of glassy crystallites occurred along with entrapped gases [7] and this caused the steady increase in linear shrinkage. However, as the Talc content increased from 2 %, reduction of sintering temperature occurs and this inhibits shrinkage, although this phenomenon does not apply to Talc contents above 6%. In other words, fluxing impact cannot resist linear shrinkage below 6% Talc as demonstrated in Figure 4 (a). From Figure 4 (b), bulk density slightly reduced as the Talc content increased from 0 to 10 % as a result of the effect of the fluxing characteristics of the Talc which reduced the sintering temperature. Although the reduction in the sintering temperature at 1000°C did not favor densification, The densification was so rapid at 1200°C and subdued the lowering of sintering temperature induced by the increasing Talc content.

Reduction in volume caused dimensional reduction viz-a-vis linear shrinkage as well as the enhanced densification noticed in the produced porcelain insulators at 1200°C. Figure 4 also revealed that the 10% Talc concentration offered the least linear shrinkage and highest bulk density at 1200°C.

It is noteworthy that total linear shrinkage increased from 8.13 % in the feldspar-rich recipe to 10.13 % in the 10 % talc substitution thereby leading to 19.75 % increase in total linear shrinkage.



(a)



(b)

Fig. 4. Total linear shrinkage (a) and bulk density (b) of PPE insulator as functions of firing temperature at 1000 and 1200°C

Likewise, bulk density increased from 1.76 % in the feldspar-rich recipe to 1.94 % in the 10% talc substitution leading to a 9.48 % rise in bulk density. This declining linear shrinkage with increase in bulk density due to pore volume reductions at 1200°C were also reported in other studies [7].

3.4 Thermal analysis

The DTA/TGA curves in Figure 5 presents the simultaneous weight loss with rise of firing temperature in real time for the produced porcelain insulator. The DTA/TGA curves demonstrated the physico-chemical transformation regime that occur during a typical kaolin calcination through endothermic and exothermic reactions as shown in Figure 5.

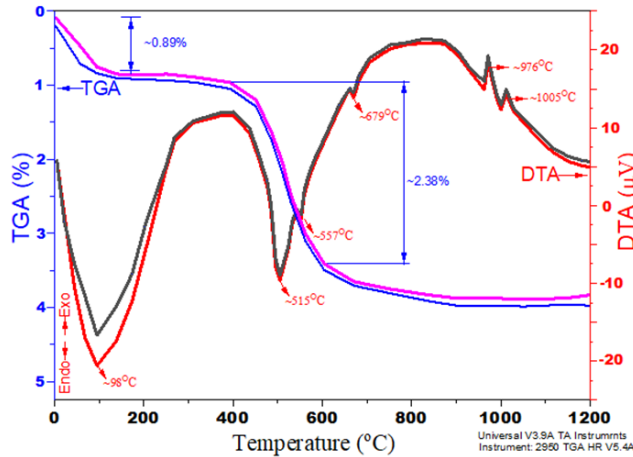
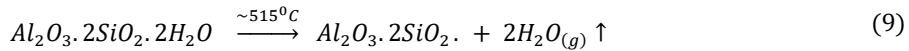
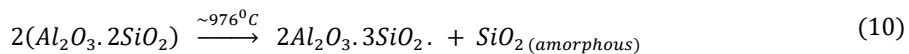


Fig. 5. Thermal profile (TGA/DTA) of produced porcelain insulator

From Figure 5, the first endothermic peak occurred at -98°C and can be attributed to the release of surface bound water in line with [20] with approximately 0.89 % weight loss indicated by the TGA curve. The second endothermic peak occurred at -51°C and is linked to the dehydroxylation of kaolinite by the removal of structural hydroxyl groups which reorganized the octahedral layers of the kaolin into the tetrahedral configuration of metakaolin. This resulted in a corresponding weight loss of 2.38 %. The dehydroxylation of kaolinite occurred until 772.8°C in the study of [19], 448.8°C in [21], 553°C in [22] and 569°C in [23]. These discrepancies can be linked to the differing raw materials, differences in processing methods, as well as ambient conditions. The total weight loss of in the porcelain body in this study was 3.27 %; consisting of 0.89% from loss of physically bound water and 2.38 % loss of chemically bound water during the decomposition of the porcelain clays. The dehydroxylation of kaolinite is the first chemical transformation in the porcelain production, this thermal reaction is represented by Eq. 9 [19, 24].

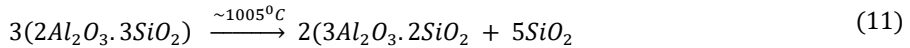


Furthermore, an endothermic peak occurred at 557°C which can be linked to the polymorphic transformation of α to β of quartz. This allotropic phase transition was also reported at 573°C in both [20] and [22]. These reductions in thermal reactions can be attributed to the fluxing properties of Talc used as a replacement of Feldspar in this study. The last noticeable endothermic peak was seen at 679°C which was linked to the sharp change at the onset of sintering and formation of glassy crystallites in the porcelain body. Then, the first noticeable exothermic peak was clear at 976°C corresponding to Al-Si spinel crystallization from the metakaolin and/or other amorphous Si-containing $\gamma\text{-Al}_2\text{O}_3$. This was reported at 999.6°C in [22] which still maintained the fluxing functions of Talc in the porcelain body. Meanwhile, this was the second thermophysical reaction and is represented by Eq 10 [19, 24].

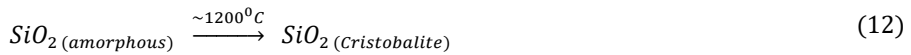


Finally, the expansive nucleation of mullite from the further decomposition of kaolin was seen to earlier commence at 1005°C similar to the study in [23] which occurred at 1050°C and 1084°C in [25].

This establishes the potentials of Talc as a fluxing replacement of Feldspar in porcelain formulation and the corresponding reaction is represented in Eq. 11 [19, 24].



Finally, the gradual rise in densification as the temperature approached 1200°C can be linked to the crystallization of stable crystals like cristobalite from the amorphous quartz and seepage of mullite melts into the porcelain pores as illustrated in Eq. 12 [19, 24].



These results demonstrate that the thermal behavior of the porcelain body was consistent with its mineralogical transformations. According to the TGA/DTA thermal profiles (Figure 5), mullite nucleation which fills up micropores and cristobalite crystallization which occurred at 1005°C and 1200°C, respectively, were volumetric reduction mechanisms. In addition, Figure 6 shows the thermal conductivity of the produced porcelain insulator which indicates the allowable heat flux that the insulator can withstand. This allowable heat flux is a significant measure of its thermal and electric shock resistance.

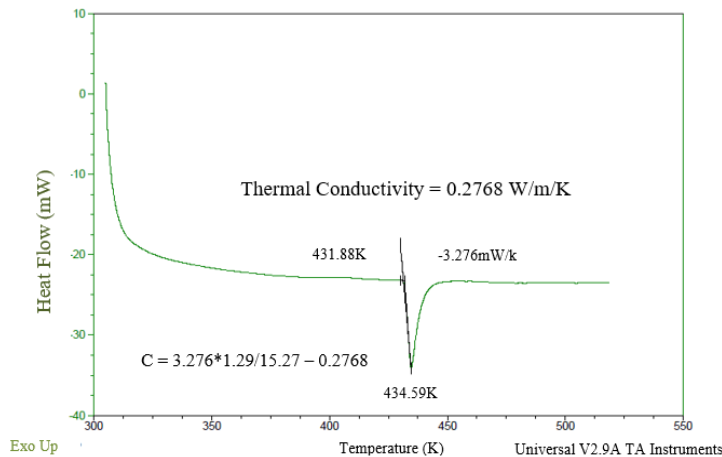


Fig. 6. Thermal conductivity (DSC) of the produced porcelain insulator

Figure 6 shows that the thermal conductivity measured from the differential scanning calorimetric analysis reveals a thermal conductivity of 0.2768 W/mK. This low thermal conductivity or high thermal resistivity demonstrates the insulator’s thermal stability under harsh temperature conditions and as well as capacity to withstand thermal shocks. This thermal stability can be linked to the 13.21% flux content recorded in the starting materials which was higher than the recommended threshold of 12% recorded in [18] for porcelain insulator production.

3.5 Microscopic evaluation

The microstructural analysis of the produced porcelain insulator was presented in Figure 7 which agrees with the chemical analysis of the raw minerals in table 2 and the properties of the produced insulator in figures 2-6. In figure 7, A = Albite; PM = Primary Mullite; P = Pores; C = Cristobalite; SM = Secondary Mullite; M = Microcline. Figure 7 demonstrated the components of the Feldspar bedrock being more of potash Feldspar than soda Feldspar.

The potash enrichment was revealed in the microcline with a characteristic green colour while its soda

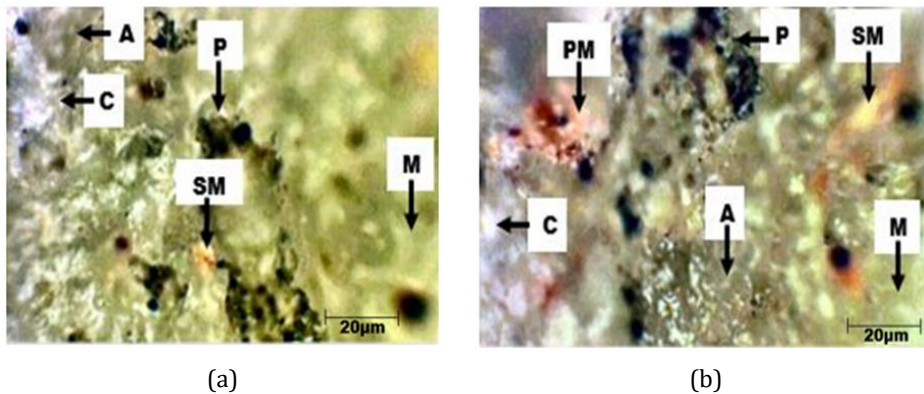


Fig. 7. Microstructural evaluation of the PPE insulator (a) No Talc (b) 10% Talc at 1200°C

Feldspar represented as albite can be distinctively seen as gray colors. The Talc-rich sample was rich in both the greenish Microcline (M) and gray Albite (A) due to the relative abundance of Feldspar in Figure 7 (a) than the Talc rich Figure 7 (b).

The Talc in Figure 7 (b) had more thermal effect than mineralogical contribution to the porcelain properties. Instead, Figure 7 (b) shows richer contents of brownish Primary Mullite (PM) and golden Secondary Mullite (SM). The glassy Cristobalite (C) was more in the Talc enriched porcelain (Figure 7 (b)) than the Feldspar dominated Figure 7 (a). The gray Albite was significant in Figure 7 (b) while the greenly microcline reduced despite the reduction of their source (Feldspar) in the porcelain (Figure 7 (b)). This will be investigated in subsequent studies. Closed Pores (P) were seen as dark regions which are present in both microstructures. According to [8], the amount of crystalline mullite and glassy phases generated during kiln firing of porcelain insulators control the dielectric strength of the insulators which should be moderate to avoid ionic conductions that will reduce the insulating propensities of the insulator. Since, the substitution of Feldspar with Talc led to more mullite and glassy cristobalite, the dielectric strength of the produced porcelain insulator with the presence of Talc in comparison with the sample without Talc as discovered in this study. In addition, the higher densification due to Talc content can also be linked to the earlier mullite transformations and their seepage into the porcelain pores. In line with table 2, apart from Alumina and Silica as the fundamental components of clay minerals, the next components were Potash and Soda with Potash being higher showing that the raw Feldspar used was alkali in nature. According to [26], Feldspar's alkalinity increases porcelain vitrification and melt's fluidity leading to unrestricted and rapid nucleation of crystals. In this light, the high fluidity enhances permeation into micropores leading to reductions in both porosity and water absorption with higher densification as recorded in figures 3. As a partial replacement of Feldspar, Talc has acted as both a fluxing agent and as a filler that displaces interconnected pores. This dual purpose is responsible for the 76.02 and 78.29 % reductions in apparent porosity and water absorption respectively.

3.6 Electrical Analysis

To investigate the effect of Feldspar replacement with Talc in electro-porcelain insulators, the electrical properties of the insulators produced was tested and the results are

presented in Table 3. The inception voltage can be defined as the minimum voltage loading at which a partial electric current is discharged through the insulator. The withstand voltage is the permissible voltage the insulator material can resist in static air at room temperature up to three minutes, while the breakdown voltage is a measure of the least voltage that can collapse the insulator's current resisting ability. Table 3 shows satisfactory voltage and current results as compared to IEC 60168 standards. Their break down voltage of 20 kV shows that they cannot be suitable for 22 kV and higher transmission lines while a withstand voltage of 14 kV shows their electrical capacity for 11 kV insulation. In addition, the glazed surface offers self-cleaning properties against dust, acid rain, high humidity and other environmentally adverse effects. Being made from local raw materials provides cost effectiveness and simplicity in production and installation. Hence, they can find wide application in 11 kV power distribution and sub-transmission lines, that is, they are ideal for all distribution lines and low voltage sub-transmission lines. Therefore, the aim of producing a low-voltage electro-porcelain insulator with Talc modified properties was successfully achieved.

In this study, electrically insulating and thermally stable porcelain insulator was produced from Nigerian local minerals by substituting its Feldspar content with Talc. The effect of sintering temperatures at 1000 °C and 1200 °C was studied. Locally sourced minerals from of Nigerian origin obtained as lumps were pulverized into homogenized powders through ball milling with a slurry made after adding 2g of Na₂SiO₃ to inhibit flocculation of suspended solids and resulting to suitable slip for casting the porcelain.

Table 3. Electric test results

Description	Voltage (kV)	Leakage Current (mA)	Remarks
Inception	10.2	0.2	Satisfactory
Withstand	14	1.2	Satisfactory
Breakdown	20	2	Satisfactory

4. Conclusion

The kaolin, ball clay and silica contents were fixed at 40 %, 10 % and 25 % respectively, with the remaining 25 % Feldspar partially replaced with Talc for each formulation. Results showed a linear relationship between porosity and firing temperature at 1200°C. There was also a direct relationship between apparent porosity and water absorption such that increase in apparent porosity gave rise to higher water ingress. Linear shrinkage and bulk density were also linearly related to the working temperature. Interestingly, the 10% replacement of Feldspar with Talc offered the least porosity, water absorption and linear shrinkage but highest bulk density all at 120 °C. Also, at this recipe, an insulator thermal conductivity of 0.2768 W/mK was obtained. This low thermal conductivity or high thermal resistivity demonstrates the insulator thermal stability under elevated temperature and as well as capacity to withstand thermal shocks. At these optimal conditions, the microstructural evaluation revealed that the 10 % Talc at 1200°C was enriched with a glassy phase, primary and secondary mullite and other crystalline phases like cristobalite, albite and microcline as well as albite but with micropores evident in both Talc and Feldspar recipes. Thermal profile of the produced insulator showed four endothermic and two exothermic peaks where mineralogical transformations validated the microstructural results in addition to weight loss and thermal conductivity results. Since the produced porcelain insulator was thermally stable up to 1200°C, the potentials of Talc as a cheap substitute of Feldspar in porcelain production is substantiated. Also, electrical performance of the porcelain insulator was rated satisfactory with Inception, Withstand and Breakdown Voltages of 10.2 kV, 14 kV and 20 kV respectively and at leakage currents

of 0.2 mA, 1.2 mA and 2 mA, respectively. Despite reduction in working temperature due to the introduction of Talc, these electrical properties demonstrate the insulator's potentials for use in distribution lines and low voltage sub-transmission lines. The potentials of Talc and other local flux materials as a cheap substitute for Feldspar in the production of porcelain insulators for high voltage transmission lines can be achieved which are within our considerations for future work. Generally, the use of the local materials and the recipe from this study would reduce importation, the costs of raw materials and energy in production. These prospects will be easier to realize if collaborations between industry and academia is enhanced especially in the country of this research. For instance, this study was funded by the personal contribution of funds by the authors, hence the study was limited to the tests reported. Future studies will encompass microscopic and spectroscopic examinations of the locally produced insulators.

References

- [1] Yang D, Cao B, Li Z, Yang L, Wu Y, On-line monitoring, data analysis for electrolytic corrosion of ± 800 kV high, International Journal of Electrical Power and Energy Systems, 2021; 131(107097). <https://doi.org/10.1016/j.ijepes.2021.107097>
- [2] Kim T, Lee Y, Sanyal S, Woo J, Choi I, Yi J, Mechanism of Corrosion in Porcelain Insulators and Its Effect on the Lifetime, Applied Science, 2020; 10(423). <https://doi.org/10.3390/app10010423>
- [3] Rojas HE, Pérez CD, León AF, Cantor LF, Electrical performance of Distribution insulators with chlorella vulgaris growth on its surface, Ingeniería e Investigación, 2015; 35(1):21-27. <https://doi.org/10.15446/ing.investig.v35n1Sup.53578>
- [4] Salem A, Rahisham A, Waheed G, Samir A, Salem A, Prediction Flashover Voltage on Polluted Porcelain Insulator Using ANN, Computers, Materials & Continua Tech Science Press, 2021; 68(3). <https://doi.org/10.32604/cmc.2021.016988>
- [5] Hsieh M, Chen W, Hsu C, Wu C, High-voltage insulation and dielectric properties of ceramic-glass composites, Journal of Asian Ceramic Societies, 2022; 10(3): 739-743. <https://doi.org/10.1080/21870764.2022.2123522>
- [6] Belhoucheta K, Bayadia A, Belhouchetb H, Maximina R, Improvement of mechanical and dielectric properties of porcelain insulators using economic raw materials, Boletín De La sociedad Sociedad Espanola De Ceramica Y Vidrio, 2019; 58: 28-37. <https://doi.org/10.1016/j.bsecv.2018.05.004>
- [7] Tullu AM, Terfasa TT, Zerfe EA, Tadese M, Beyene E, Abebe AM, Adoshe DM, Effect of cullet on firing temperature and dielectric properties of porcelain insulator, Heliyon, 2022; 8(2). <https://doi.org/10.1016/j.heliyon.2022.e08922>
- [8] Beyene E, Tiruneh SN, Andoshe DM, Abebe AM, Tullu AM, Partial substitution of Feldspar by alkaline-rich materials in the electrical porcelain insulator for reduction of processing temperature, Materials Research Express, 2022. 9. <https://doi.org/10.1088/2053-1591/ac7301>
- [9] Sanz J, Tomasa O, Jimenez-Franco A, Sidki-Rius N, Talc. In: Elements and Mineral Resources, 2022; 391-393. https://doi.org/10.1007/978-3-030-85889-6_98
- [10] Abdel-Rahman AM, El-Desoky HM, Shalaby BNA, Awad HA, Ene A, Heikal MA, El-Awny H, Fahmy W, Taalab SA, Zakaly HMH, Ultramafic Rocks and Their Alteration Products From Northwestern Allaqi Province, Southeastern Desert, Egypt: Petrology, Mineralogy, and Geochemistry. Front. Earth Sci., 2022; 10. <https://doi.org/10.3389/feart.2022.894582>
- [11] Baba AA, Ibrahim AS, Bale RB, Adekola FA, Alabi AGF, Purification of a Nigerian Talc ore by acid leaching. Applied Clay Science, 2015; 114: 476-483. <https://doi.org/10.1016/j.clay.2015.06.031>
- [12] Olajide-Kayode JO, Okunlola OA, Olatunji AS, Compositional Features and Industrial Assessment of Talcose Rocks of Itaganmodi-Igun Area, Southwestern Nigeria, Journal

- of Geoscience and Environment Protection, 2018; 6: 59-77
<https://doi.org/10.4236/gep.2018.61005>
- [13] Emmanuel S A, Physicochemical Evaluation of Some Talc Mineral Deposits Collected From Four States In Nigeria, Journal of Chemical Society of Nigeria, 2022; 47(4): 712 - 717. <https://doi.org/10.46602/jcsn.v47i4.779>
- [14] Mgbemere HE, Obidiegwu EO, Oginni AA, Production and Characterisation of Porcelain Insulator Modified with Talc and Bentonite, Nigerian Research Journal of Engineering and Environmental Sciences, 2020; 5(2): 659-671.
- [15] ASTM C20-00, Standard Test Methods for Apparent Porosity, Water Absorption, Apparent Specific Gravity and Bulk Density of Burned Refractory Brick and Shaped by Boiling Water, ASTM International, 2015.
- [16] ASTM C356-17, Standard Test Method for Linear Shrinkage of Preformed High Temperature Thermal Insulation Subjected to Soaking Heat, ASTM International, 2017.
- [17] Nwachukwu VC, Lawal SA, Investigating the Production Quality of Electrical Porcelain Insulators from Local Materials, IOP Confer. Ser.: Materials Science and Engineering, 2018; 413(012076). <https://doi.org/10.1088/1757-899X/413/1/012076>
- [18] Moyo MG, Park E, Ceramic Raw Materials in Tanzania - Structure and Properties for Electrical Insulation Application, International Journal of Engineering Research & Technology, 2014; 3 (10).
- [19] Xu X, Lao X, Wu J, Zhang Y, Xu X, Li K, Microstructural evolution, phase transformation, and variations in physical properties of coal series kaolin powder compact during firing, Applied Clay Science, 2015; 115: 76-86. <https://doi.org/10.1016/j.clay.2015.07.031>
- [20] Hernandez MF, Violini MA, Serra MF, Conconi MS, Suarez G, Rendtorff MN, Boric acid (H₃BO₃) as flux agent of clay-based ceramics, B₂O₃ effect in clay thermal behavior and resultant ceramics properties, Journal of Thermal Analysis and Calorimetry, 2020; 139:1717-1729. <https://doi.org/10.1007/s10973-019-08563-4>
- [21] Shanjun K, Yanmin W, Zhidong P, Chengyun N, Shulong Z, Recycling of polished tile waste as a main raw material in porcelain tiles, Journal of Cleaner Production, 2016; 115: 238-244. <https://doi.org/10.1016/j.jclepro.2015.12.064>
- [22] Valmir J, Michelle F, Wherlyson PG, Romualdo R, Gelmires A, Hélio L, Lisiane N, Porous mullite blocks with compositions containing kaolin and alumina waste, Ceramics International, 2016; 42(14): 15471-15478. <https://doi.org/10.1016/j.ceramint.2016.06.199>
- [23] Garcia-Valles M, Alfonso P, Martínez S, Núria R, Mineralogical and Thermal Characterization of Kaolinitic Clays from Terra Alta (Catalonia, Spain). Minerals, 2020; 10: 142. <https://doi.org/10.3390/min10020142>
- [24] Krupa P, Malinarič S, Thermal Properties of green alumina porcelain. Ceramics International, 2015; 41: 3254-3258. <https://doi.org/10.1016/j.ceramint.2014.11.015>
- [25] De Aza AH, Turrillas X, Rodriguez MA, Pena DP. Time-resolved powder neutron diffraction study of the phase Transformation sequence of kaolinite to mullite. Journal of the European Ceramic Society, 2014; 34: 1409-1421. <https://doi.org/10.1016/j.jeurceramsoc.2013.10.034>
- [26] Njoya, D, Tadjuidje FS, Ndzana EJA, Pountouonchi, A., Tessier-Doyen, N., and Lecomte-Nana, G. Effect of Flux Content and Heating Rate on The Microstructure and Technological Properties of Mayouom (Western-Cameroon) Kaolinite Clay Based Ceramics. Journal of Asian Ceramic Societies, 2017; 5 (4): 422-426. <https://doi.org/10.1016/j.jascer.2017.09.004>